Reactivity of a Borane Appended 1,1'-Bisphosphinoferrocene Ligand: Transition Metal and Lewis Acid Coordination, Cyclopentadienyl Ring Borylation, and Boronium Cation Generation

Bradley E. Cowie, David J. H. Emslie*

Department of Chemistry and Chemical Biology, McMaster University, 1280 Main Street West, Hamilton, Ontario, L8S 4M1, Canada.

Supporting Information Placeholder

ABSTRACT: The reaction of a borane-appended analogue of 1,1'-bisphosphinoferrocene, [Fe(η^5-$C_5H_4PPh_2$)(η^5-$C_5H_4P^tBu${(*o*-BPh_2)C_6H_4})] (FcPPB), with [$W(CO)_6$] under photochemical conditions lead to [$W(CO)_4$(FcPPB*)] (**1**) (FcPPB* = [Fe(η^5-$C_5H_4PPh_2$){η^5-$C_5H_3P(^tBu)C_6H_4$-*o*-BPh}]), in which the borane has added to a cyclopentadienyl ring of the ligand backbone and benzene has been eliminated. Formation of **1** does not occur under thermal conditions, and benzene solutions of the free FcPPB ligand are unreactive under both photochemical and refluxing conditions. Boranes of greater Lewis acidity than the pendent triarylborane of FcPPB were introduced to free FcPPB in an effort to promote intramolecular electrophilic borylation of the ferrocene backbone by eliminating the borane-phosphine interaction in FcPPB. However, addition of $B(C_6F_5)_3$ provided [Fe(η^5-$C_5H_4PPh_2${$B(C_6F_5)_3$})(η^5-$C_5H_4P^tBu${$C_6H_4(BPh_2)$-*o*})], FcPPB{$B(C_6F_5)_3$} (**2**), in which $B(C_6F_5)_3$ forms an adduct with the –*P*Ph_2 group, and the intramolecular phosphine–borane interaction present in free FcPPB is maintained in **2**. Furthermore, addition of two equiv. of $BF_3(OEt_2)$ to FcPPB yielded a single diastereomer of [Fe(η^5-$C_5H_4PPh_2$)(η^5-$C_5H_4P^tBu${C_6H_4(BPh-*o*})][BF_4] (**3**), in which one *B*-phenyl substituent has been abstracted to generate a boronium cation {$BR_2L_2^+$}. Reaction of FcPPB with [$AuCl(PPh_3)$]/$GaCl_3$ afforded dimetallic [{Au(FcPPB)}$_2$][$GaCl_4$]$_2$ (**4**) as a mixture of diastereomers featuring μ-1κ*P*:2κ*P'*-coordination of each FcPPB ligand, and a near linear geometry at each gold(I) center. The pendent borane in **4** interacts only weakly or not at all with gold, but electrophilic addition of the borane to the ferrocene backbone was not observed upon UV irradiation.

INTRODUCTION

Ambiphilic ligands are defined as those containing a combination of Lewis basic and Lewis acidic sites, and the first crystallographically characterized example of an ambiphilic ligand complex featuring a transition metal–group 13 Lewis acid interaction was reported by Hill *et al.* in 1999.[1] Since then, ambiphilic ligands have been coordinated to a broad range of late transition metals,[2] and in this field the Emslie group's research has focused on the TXPB,[3] FcPPB[4,5] and FcPPAl[6] ligands (a-c in Figure 1). The latter are group 13 Lewis acid appended analogues of dppf {1,1'-bis(diphenylphosphino)ferrocene}, and were developed to overcome limitations associated with the lability of the thioether donor of TXPB, as well as to introduce increased flexibility in the bite angle between the two donor atoms. In all three ambiphilic ligands (TXPB, FcPPB and FcPPAl), the Lewis acid is located in a terminal position within the donor/acceptor array, potentially increasing the accessibility of the Lewis acid for interaction with co-ligands and external substrates. This positioning of the Lewis acid contrasts that in other tridentate and tetradentate ambiphilic ligands such as ^{R}DPB^{Ar},[7] ^{R}TPB,[8] and B(mt^{tBu})$_3$[1] (d-f in Figure 1), in which the Lewis acid occupies a central position.

In the chemistry of FcPPB, reaction with [$Pt(nb)_3$] (nb = norbornene),[4] [$Pd_2(dba)_3$] (dba = *trans*,*trans*-dibenzylideneacetone), or [$Ni(COD)_2$] (COD = 1,5-cyclooctadiene)[5] afforded [M(FcPPB)] (M = Pt, Pd or Ni) in which the metal is coordinated to both phosphine donors of FcPPB, and engages in an η^3*BCC*-interaction with the arylborane, via boron and the *ipso* and *ortho* carbon atoms of one *B*-phenyl ring. The platinum complex, [Pt(FcPPB)] reacted with CO to form [Pt(CO)(FcPPB)] in which the borane is η^2*BC*-coordinated, and with CNXyl to form [Pt(CNXyl)(FcPPB)] in which the borane is η^1*B*-coordinated, highlighting the range of coordination modes accessible to the arylborane in FcPPB. Additionally, H_2 and HC_2Ph underwent oxidative addition with [Pt(FcPPB)], generating [Pt(R)(μ-H)(FcPPB)] (R = H or C_2Ph) in which a hydride ligand bridges between platinum and boron. However, whereas the former complex is thermally robust, the acetylide complex underwent rapid room temperature rearrangement to form the unexpected vinylborane complex, [Pt(FcPPB')] (FcPPB' = [Fe(η^5-$C_5H_4PPh_2$)(η^5-$C_5H_4P^tBu${C_6H_4(BPh-CPh=CHPh-*Z*)-*ortho*}]), which slowly isomerized to afford a mixture with a complex in which platinum is coordinated to the opposite face of the vinylborane.[4]

To extend the chemistry of FcPPB, we were motivated to explore reactions with homoleptic transition metal carbonyl complexes in which M–BR_3 and M–X–BR_3 (X = an anionic ligand) interactions are precluded, and M–(CO)–BR_3 bridging interactions may be observable. Complexes featuring such interactions have not previously been isolated. However, Lewis acids are known to greatly increase the rate of various carbonyl

ligand insertion reactions, and to facilitate otherwise thermodynamically-unfavorable insertion reactions between late transition metal-bound CO and hydride or perfluoroalkyl ligands.[9,10]

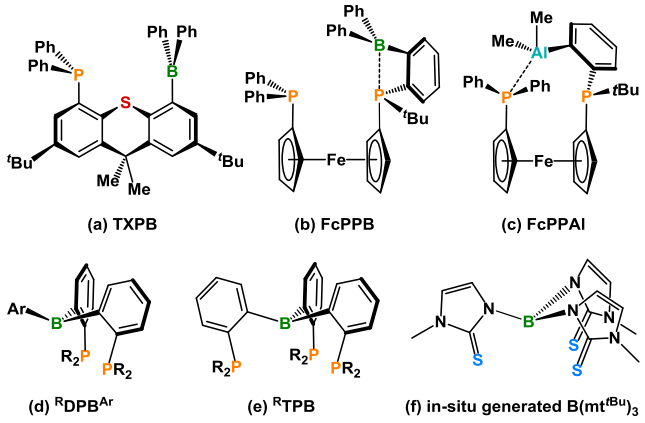

Figure 1. Selected tridentate and tetradentate ambiphilic ligands (R = ^{i}Pr or Ph; Ar = Ph or Mesityl).

Herein we describe the reaction of FcPPB with [W(CO)$_6$] under photolytic conditions, which afforded the unanticipated product of κ^2*PP*-coordination to tungsten, borane electrophilic addition to the proximal cyclopentadienyl ring of FcPPB, and subsequent benzene elimination. Consequently, the reactions of FcPPB with B(C$_6$F$_5$)$_3$, BF$_3$(OEt$_2$), and [Au(PPh$_3$)][GaCl$_4$] were carried out in an effort to probe whether the aforementioned electrophilic borylation reactivity is a common reactivity trait of FcPPB, once the phosphine–borane interaction in the free ligand has been disrupted and the borane is only weakly- or non-coordinated. These reactions afforded an FcPPB–borane adduct, a boronium cation, and a dimetallic gold complex with little or no interaction between gold and the pendent boranes.

RESULTS AND DISCUSSION

UV irradiation of a solution of FcPPB and [W(CO)$_6$] provided [W(CO)$_4$(FcPPB*)] (**1**; FcPPB* = [Fe(η^5-C$_5$H$_4$PPh$_2$){η^5-C$_5$H$_3$P(^{t}Bu)C$_6$H$_4$-*o*-BPh}] as an orange solid in 82% yield (Scheme 1). Coordination of the both phosphine donors to tungsten was evidenced by signals at 19.7 and 14.2 ppm in the ^{31}P{^{1}H} NMR spectrum, with $^1J_{31P,183W}$ coupling of 233 and 236 Hz and a *cis*-$^2J_{31P,31P}$ coupling of 24 Hz. However, the cyclopentadienyl region of the ^{1}H NMR spectrum integrated to seven protons, as opposed to eight, and the ^{11}B NMR signal was observed at 57 ppm, indicative of a free or only weakly-coordinated borane.

X-ray quality crystals of **1**·C$_6$H$_6$ were obtained by slow diffusion of hexanes into a benzene solution of **1** at room temperature, and revealed that the triarylborane in FcPPB has been converted to a diarylferrocenylborane. Boron is now bound to the proximal cyclopentadienyl ring of the ferrocene backbone and one cyclopentadienyl hydrogen atom and one *B*-phenyl ring have been eliminated as benzene (Figure 2). The W–P(1) and W–P(2) bond lengths in **2** are 2.569(1) and 2.572(1) Å, respectively, and the tungsten center adopts a distorted octahedral geometry with *cis* and *trans* L–W–L (L = CO or PR$_3$) angles ranging from 82.03(9)-97.73(3)° and 169.1(1)-178.5(1)°, respectively; the P(1)–W–P(2) bite angle is 97.73(3)°.

Scheme 1. Synthesis of [W(CO)$_4$(FcPPB*)] (**1**) from FcPPB and [W(CO)$_6$].

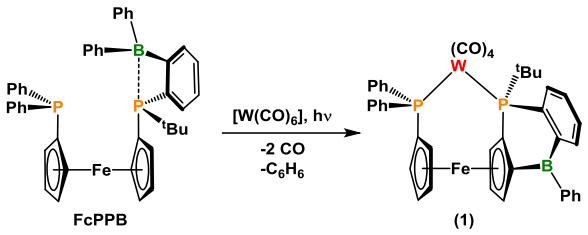

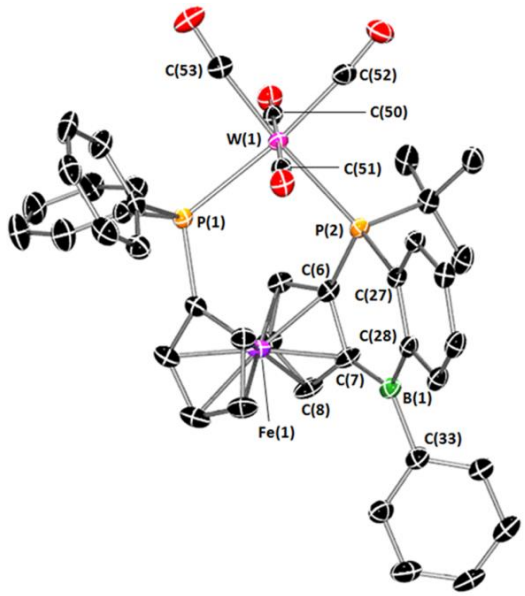

Figure 2. Solid-state structure of [W(CO)$_4$(FcPPB*)]·C$_6$H$_6$ (**1**·C$_6$H$_6$) with ellipsoids at 50% probability. Hydrogen atoms and lattice solvent are omitted for clarity. Selected bond lengths [Å] and angles [°]: W(1)–P(1), 2.569(1); W(1)–P(2), 2.572(1); B(1)–C(7), 1.533(5); B(1)–C(28), 1.572(5); B(1)–C(33), 1.567(5); P(1)–W(1)–C(52), 169.1(1); P(2)–W(1)–C(53), 174.0(1); C(51)–W(1)–C(50), 178.5(1); P(1)–W(1)–P(2), 97.73(3); C(7)–B(1)–C(28), 118.7(3); C(7)–B(1)–C(33), 120.1(3); C(28)–B(1)–C(33), 121.2(3).

Boron is trigonal planar, with the sum of the C-B-C angles equal to 360.0(5)°, and the B–C(7) bond length is 1.533(5) Å. Similar values were reported for the borane-substituted ferrocenes [Fe(η^5-C$_5$H$_4$BPh$_2$)(η^5-C$_5$H$_5$)][11] and [Fe{η^5-C$_5$H$_4$B(*o*-tol)$_2$}(η^5-C$_5$H$_5$)],[12] as well as the 1,1'-phosphine/borane-disubstituted ferrocene [Fe(η^5-C$_5$H$_4$PPh$_2$)(η^5-C$_5$H$_4$BMes$_2$)][13] (Mes = 2,4,6-Me$_3$C$_6$H$_2$). At 1.533(5) Å, the B–C(7) bond in **1** is shorter than the B–C$_{aryl}$ bond distances {B–C(28) = 1.572(5) Å; B–C(33) = 1.567(5) Å}, indicative of superior π-donation to boron from the cyclopentadienyl ring, relative to the phenyl groups. Furthermore, borafulvene-type distortions are observed within the cyclopentadienyl ring; in particular, the C(7)–C(6) and C(7)–C(8) bond lengths are 1.443(5) and 1.446(5) Å, while the remaining three C–C bond lengths range from 1.406(5)–1.426(5) Å. Similar distortions have been reported for the aforementioned literature examples of borane-substituted ferrocenes, and

in all cases the longest C–C bond lengths are observed between C_{ortho} and C_{ipso} of the borane-substituted cyclopentadienyl ring.

A notable feature of **1** is the degree of bending of the ferrocenyl-borane towards the iron center. Wagner and co-workers have investigated this feature in a series of borane-substituted ferrocenes, and concluded that bending of the borane towards iron is due to a bonding interaction between the iron d_{x2-y2} orbital and the C_{ipso}–B π-system, a delocalized through-space interaction involving the C_{ipso}–B π-system and the other Cp-ring, and electrostatic interactions which depend critically on the presence of the other Cp-ring. The degree of bending of the ferrocenyl-borane towards iron is referred to as the dip angle, α*, which is obtained by subtracting α from 180° (α = Cp_{cent}–C_{ipso}–B; Cp_{cent} = centroid of the borane-substituted cyclopentadienyl ring), and decreases as the Lewis acidity of the borane unit decreases.[11,14,15] Complex **1** possesses a dip angle of 12°, which is in good agreement with the aforementioned borane-substituted ferrocenes [Fe(η^5-$C_5H_4BPh_2$)(η^5-C_5H_5)] and [Fe{η^5-$C_5H_4B(o\text{-}tol)_2$}(η^5-C_5H_5)] (α* = 13 and 8°, respectively), but is smaller than α* for [Fe(η^5-$C_5H_4BBr_2$)(η^5-C_5H_5)] (α* = 17.7, 18.9°)[15] and [Fe{η^5-$C_5H_4B(C_6F_5)_2$}(η^5-C_5H_5)] (α* = 16°),[16] in accordance with the inferior Lewis acidity of the pendent borane in **2**.

Scheme 2. Proposed mechanism for intramolecular electrophilic borylation of the ferrocene backbone of FcPPB, resulting in conversion of FcPPB to FcPPB*.

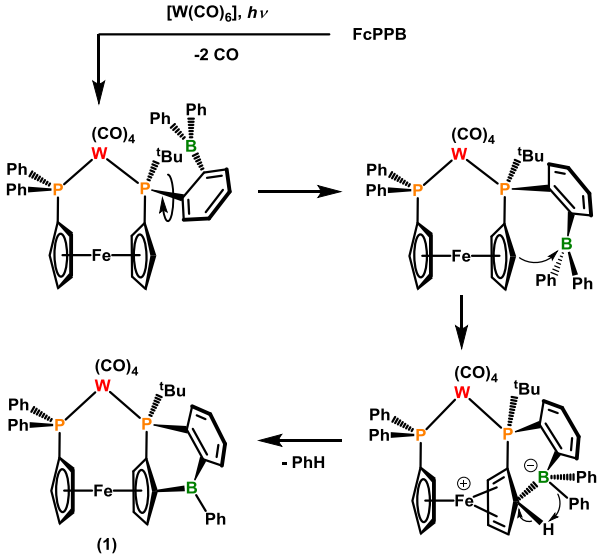

The synthesis of **1** only proceeded under photochemical conditions; no reaction took place when a benzene solution of FcPPB and [W(CO)$_6$] was heated to 80 °C for 24 hours. Examples of direct electrophilic borylation of a metallocene cyclopentadienyl ring are quite prevalent in the literature. However it has typically been achieved through the use of highly Lewis acidic boranes, such as BX_3 (X = Cl, Br, I), B_2Cl_4, $HBCl_2$, $RBBr_2$ (R = Me, Ph), $B(C_6F_5)_3$, and $HB(C_6F_5)_2$, and often requires elevated temperatures.[17] To the best of our knowledge, the reaction to form **1** is the first example of direct electrophilic borylation of ferrocene by a non-fluorinated tris(hydrocarbyl)borane.

In the reaction to form **1**, photochemical reaction conditions will promote carbonyl ligand dissociation, presumably resulting in κ^2*PP*-coordination of FcPPB. The borane in the resulting intermediate may be free or weakly coordinated to a CO co-ligand, rendering it available to electrophilically add to the adjacent cyclopentadienyl ring, followed by loss of a *B*-phenyl substituent and the Cp–H hydrogen atom as benzene, ultimately transforming the FcPPB ligand into FcPPB* (Scheme 2). In an effort to determine whether [W(CO)$_4$(dppf)] {dppf = 1,1'-bis(diphenylphosphino)ferrocene} undergoes intermolecular borylation reactivity with tris(hydrocarbyl)boranes, a benzene solution of [W(CO)$_4$(dppf)] was heated with BEt_3, BPh_3 and $B(C_6F_5)_3$ at 80 °C. However, BEt_3 and BPh_3 did not react, and $B(C_6F_5)_3$ yielded an insoluble orange precipitate which was not characterized further.

In contrast to the photochemical reactivity of FcPPB with [W(CO)$_6$], free FcPPB is unreactive under thermal and photochemical conditions, perhaps because the borane is prevented from interacting with the adjacent cyclopentadienyl ring by intramolecular phosphine-borane adduct formation. In order to probe this hypothesis, various Lewis acids were introduced to FcPPB in an attempt to displace the intramolecular phosphine-borane adduct. Neither BEt_3 or BPh_3 reacted with FcPPB, and $AlMe_3$ yielded a complex mixture of products, whereas both $B(C_6F_5)_3$ and $BF_3(OEt_2)$ reacted cleanly with FcPPB (Schemes 3 and 4, respectively).

Scheme 3. Synthesis of FcPPB{$B(C_6F_5)_3$} (**2**) via the addition of $B(C_6F_5)_3$ to FcPPB.

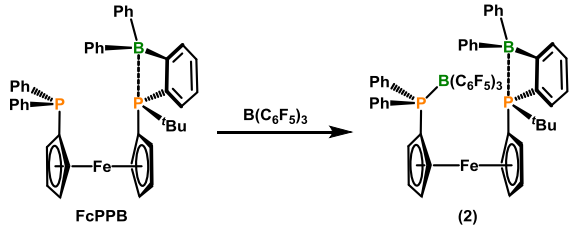

Addition of one equivalent of $B(C_6F_5)_3$ to FcPPB provided [Fe{η^5-$C_5H_4PPh_2(B(C_6F_5)_3)$}(η^5-$C_5H_4P^tBu${(*o*-BPh_2)C_6H_4})] (FcPPB{$B(C_6F_5)_3$}; **2**) in which the C_5H_4*P*Ph_2 moiety participates in adduct formation with $B(C_6F_5)_3$. However, the intramolecular adduct between the borane moiety of FcPPB and the C_5H_4*P*(^{t}Bu)Ar phosphine is maintained (Scheme 3). X-ray quality crystals of **2** proved elusive, but key spectroscopic evidence for the structure of **2** consists of: (1) a shift in the C_5H_4*P*Ph_2 ^{31}P NMR signal from –17.2 ppm in FcPPB to 20.0 ppm in **2** {a broad singlet ($\omega_{1/2}$ = 93 Hz) indicating coordination to quadrupolar boron}, (2) emergence of a signal at –4 ppm representing adducted $B(C_6F_5)_3$, and a shift in the $RBPh_2$ ^{11}B NMR signal from 17 ppm in FcPPB to 25 ppm in **2**, (3) ^{19}F NMR signals at –125.1, –156.7 and –164.3 ppm with a $\Delta_{p\text{-}m}$ value of 7.6 ppm; these signals are significantly shifted relative to those of free $B(C_6F_5)_3$, and are similar to those of Ph_3P{$B(C_6F_5)_3$},[18] and (4) eight cyclopentadienyl ^{1}H NMR signals (integrating to 1H each) in **2**, as opposed to seven in compound **1**, indicating that electrophilic addition to the adjacent Cp-ring did not occur. A second equivalent of $B(C_6F_5)_3$ was added to **2** in an attempt to promote displacement of the intramolecular P–B interaction, but this only resulted in sharpening of the singlet in the ^{31}P{^{1}H} NMR spectrum representing the $C_5H_4PPh_2$ moiety, indicating that some $B(C_6F_5)_3$ dissociation from **2** occurs in solution.

In contrast to the reaction of FcPPB with $B(C_6F_5)_3$, reaction of FcPPB with 2 equiv. of $BF_3(OEt_2)$ afforded $[Fe\{\eta^5\text{-}C_5H_4PPh_2\}(\eta^5\text{-}C_5H_4P^tBu\{o\text{-}BPh)C_6H_4\})][BF_4]$ {$[FcPPB^{-Ph}][BF_4]$; **3**} as a single diastereomer, presumably with release of $PhBF_2$; Scheme 4. Formation of **3** likely proceeds through initial exchange of a *B*-phenyl substituent in FcPPB for fluoride {perhaps via $[(\kappa^2PP\text{-FcPPB})BF_2]F$},[19] followed by abstraction of the newly installed fluoro substituent by a 2nd equivalent of BF_3 (Scheme 4).[20] Compound **3** may be described either as a boronium cation stabilized by intramolecular bisphosphine coordination (canonical form **B** in Scheme 4), or as a phosphine-coordinated borylphosphonium cation (canonical forms **A** and **C** in Scheme 4).[21]

Scheme 4. (a) Synthesis of $[FcPPB^{-Ph}][BF_4]$ (**3**) via the addition of two equivalents of $BF_3(OEt_2)$ to FcPPB. (b) Three canonical forms (A-C) describing the cationic portion of **3**.

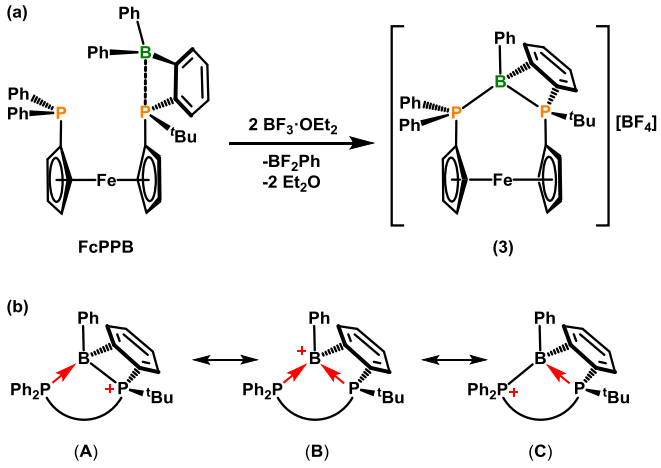

X-ray quality crystals of **3** were obtained over several days from a room temperature benzene solution of FcPPB and $BF_3{\cdot}OEt$ (2 equiv.). However, elevated yields of **3** were obtained by heating a benzene solution of the two reactants for 3 days at 70 °C, precipitating **3** as a pale orange solid in 64 % yield. The solid-state structure of **3** (Figure 3) features B(1)–P(1) and B(1)–P(2) bond lengths of 1.981(6) and 2.059(6) Å, respectively, and a P(1)–B–P(2) bite angle equal to 114.2(3)°. The B(1)–P(2) bond length in **3** is significantly shorter than the analogous bond distance in neutral FcPPB (2.146(2) Å), consistent with phosphine coordination to a cationic versus a neutral boron centre. However, both P–B bond lengths in **3** are substantially longer than those reported for the bisphosphineboronium salts $[(^tBu_2HP)_2BH_2]X$ (X = Br, P–B = 1.934(5), 1.948(5) Å; X = OTf, P–B = 1.938(2), 1.941(2) Å; X = BAr^F_4, P–B = 1.933(3), 1.936(3) Å; BAr^F_4 = $B\{C_6H_3\text{-}3,5\text{-}(CF_3)_2\}_4$),[22] $[(Et_3P)_2BH_2][B(cat)_2]$ (cat = $C_6H_4\text{-}1,2\text{-}O_2$; P–B = 1.896(6)–1.913(6) Å),[23] and $[Ni\{\kappa^2\text{-}(CH_2PMe_2)_2BMe_2\}_2]$ (P–B = 1.92(2)–1.94(2) Å),[24] due to greater steric hindrance and decreased phosphine basicity in **3**, possibly compounded by steric constraints imposed by the ligand framework. To the best of our knowledge **3** is the first intramolecular bisphosphine-stabilized boronium cation, although Bourissou *et al.* recently reported the conversion of $C_{10}H_6\text{-}1\text{-}(PPh_2)\text{-}8\text{-}(BMesBr)$ to $[C_{10}H_6\text{-}1\text{-}(PPh_2)\text{-}8\text{-}(BMes)]^+$; an intramolecular phosphine-stabilized borenium cation.[25]

Scheme 5. Potential reaction pathway for the formation of **3**.

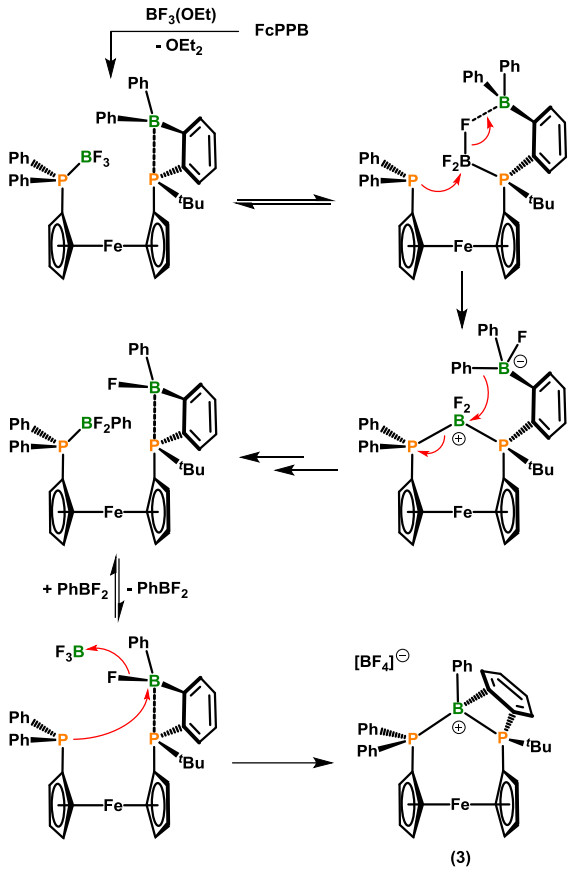

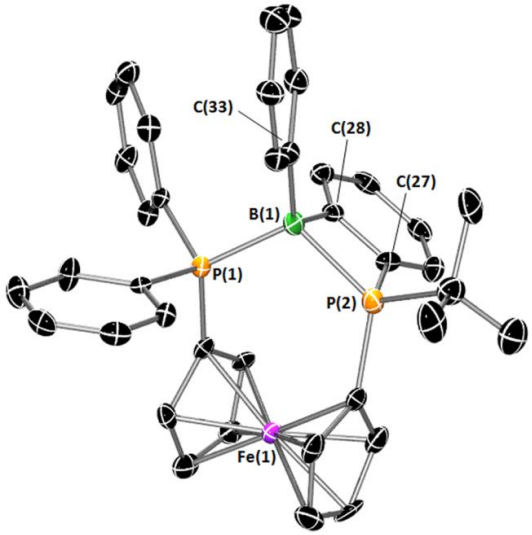

Figure 3. Solid-state structure of $[FcPPB^{-Ph}][BF_4]$ (**3**) with ellipsoids at 50% probability. Hydrogen atoms and the BF_4 counter anion are omitted for clarity. Selected bond lengths [Å] and angles [°]: B(1)–P(1), 1.981(6); B(1)–P(2), 2.059(6); B(1)–C(28), 1.626(7); B(1)–C(33), 1.590(8); P(1)–B(1)–P(2), 114.2(3); P(1)–B(1)–C(28), 107.3(4); P(1)–B(1)–C(33), 112.2(4); P(2)–B(1)–C(28), 80.9(3); P(2)–B(1)–C(33), 119.2(4); P(1)–B(1)–C(33), 112.2(4); C(28)–B(1)–C(33), 119.2(5); C(27)–C(28)–B(1), 104.7(4).

Despite its insolubility in arene solvents, compound **3** is readily soluble in CD_2Cl_2, and gave rise to ^{31}P NMR signals at 27.8 and 1.0 ppm, representing the $C_5H_4P(^tBu)Ar$ and $C_5H_4PPh_2$ phosphines, respectively, and a ^{19}F NMR signal for the BF_4 anion at –152.9 ppm. The ^{31}P NMR signals are broadened singlets with $\omega_{1/2}$ values of 65 and 150 Hz, respectively, indicative of coordination to quadrupolar boron, and are shifted to high frequency relative to those of FcPPB. The ^{11}B NMR signals are located at –1.4 and –2.0 ppm; the former is a sharp singlet representing the BF_4^- anion, and the latter is a broadened singlet ($\omega_{1/2}$ = 250 Hz) that corresponds to the boronium cation. Similar spectroscopic features were reported for the boronium cations in $[Ph_2B^-(\mu\text{-pyr})_2B^+Me_2]$ (pyr = 2-pyridyl; ^{11}B NMR = 4.0 ppm),[26] $[Fe\{\eta^5\text{-}C_5H_4BMe(\kappa^2NN\text{-}2,2'\text{-bipy})\}_2][PF_6]_2$ {^{11}B NMR = 8.5 ppm},[27] and $[BBN(L)_2][NTf_2]$ (BBN = 9-borabicyclo[3.3.1]nonyl; Tf = SO_2CF_3; $(L)_2$ = bipy or $(P^nBu_3)_2$; ^{11}B NMR = 5.2 and –5.4 ppm, respectively).[28]

In an alternative approach to access FcPPB complexes in which the borane is only weakly coordinated, FcPPB was reacted with in-situ-generated $[Au(PPh_3)][GaCl_4]$ to provide $[\{Au(FcPPB)\}_2][GaCl_4]_2$ (**4**) as a tangerine-coloured solid in 90 % yield (Scheme 6).[29] Complex **4** was obtained as a mixture of diastereomers in an approximate 3:2 ratio, giving rise to one set of ^{31}P NMR signals at 63.3 and 40.7 ppm ($^2J_{P,P}$ = 310 Hz), and a second set at 63.1 and 39.1 ppm ($^2J_{P,P}$ = 302 Hz). The magnitude of the ^{31}P-^{31}P coupling constant for each diastereomer is characteristic of *trans*-disposed phosphine ligands bound to gold,[30] and in both cases, ^1H-^{31}P-HMBC NMR spectroscopy confirmed that the higher frequency signal represents the $C_5H_4P(^tBu)Ar$ phosphine. The ^{11}B NMR chemical shift for **4** is 68 ppm, indicating that the borane in FcPPB does not engage in a strong interaction with the gold center.[31]

Scheme 6. Synthesis of $[\{Au(FcPPB)\}_2][GaCl_4]_2$ (**4**; a mixture of diastereomers) from FcPPB and $[Au(PPh_3)][GaCl_4]$.

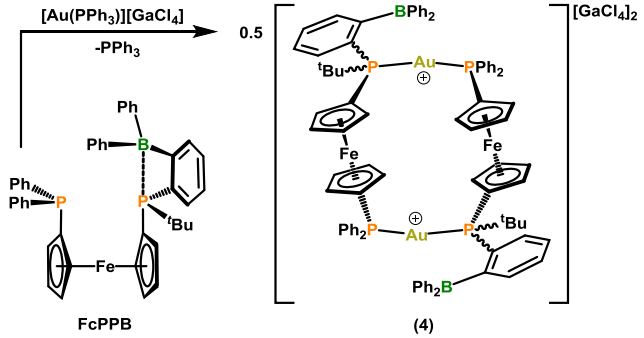

An X-ray crystal structure was obtained for *meso*-**4**·$2C_6H_{14}$ (Figure 4), revealing Au(FcPPB) units with μ-1κP:2$\kappa P'$-coordination of each FcPPB ligand, and a P(1)–Au–P(2) bond angle of 158.84(2)°. The Au–P(1) and Au–P(2) bond lengths are 2.3149(6) and 2.3178(7) Å, respectively, similar to those in other $[Au(PR_3)_2]^+$ complexes.[30,32] The two Au centers are separated by a distance of ~6.8 Å, eliminating the possibility of aurophilic interactions.[33] The geometry at boron is essentially planar [Σ(CBC) = 359.4(4)°], consistent with the high frequency ^{11}B NMR chemical shift (*vide supra*). Furthermore, the Au–B bond distance of 3.121(3) Å in **4** is significantly longer than the sum of the covalent radii (2.20 Å)[34] as well as the Au–B bond lengths reported for $[AuCl\{(o\text{-}^iPr_2P)C_6H_4BR_2\}]$ (R = Cy, Au–B = 2.90 Å; R = BFlu, BFlu = 9-boraflourenyl, Au–B = 2.66 Å),[35] $[AuCl(^RDPB^{Ph})]$ ($^RDPB^{Ph}$ = $\{(o\text{-}R_2P)C_6H_4\}_2BPh$; R = ^{i}Pr, Au–B = 2.309(8) Å; R = Ph, Au–B = 2.335(5) Å),[36] $[AuCl(^{iPr}TPB)]$ (^{iPr}TPB = $\{(o\text{-}^iPr_2P)C_6H_4\}_3B$; Au–B = 2.318(8) Å),[37] $[Au(^{iPr}TPB)][GaCl_4]$ (Au–B = 2.448 Å)[38] and $[Au(^{Ph}DPB^{Ph})][SbF_6]$ (Au–B = 2.521 Å),[39] all of which feature direct κ^1B-coordination of a pendent borane to gold. However, the Au–B bond distance in *meso*-**4** is within the sum of the Van der Waals radii (~3.75 Å),[40] and the gold center is puckered towards the borane of FcPPB, lying 0.425 Å above the centroid of the P(1)···P(2) vector, and bent at an angle of 21° towards the borane {P(1)–Au–P(2) = 158.84(2)°}, so the possibility of a weak Au–B interaction cannot be discounted. The long Au–B distance in *meso*-**4** is not structurally enforced by the ligand framework, given that a similar dimetallic structure was previously observed for $[\{Pt(FcPPAl)\}_2]$ (FcPPAl = $[Fe(\eta^5\text{-}C_5H_4PPh_2)(\eta^5\text{-}C_5H_4P^tBu\{(o\text{-}AlMe_2)C_6H_4\})]$), featuring a short Pt–Al distance of 2.482(1) Å.[6]

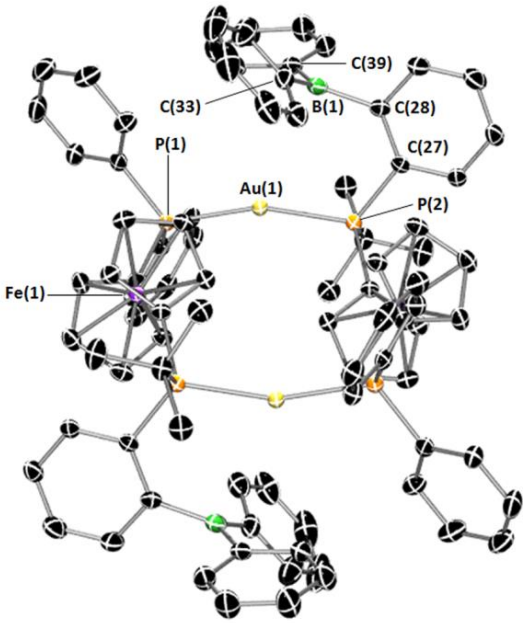

Figure 4. Solid-state structure of *meso*-$[\{Au(FcPPB)\}_2][GaCl_4]_2\cdot 2C_6H_{14}$ (*meso*-**4**·$2C_6H_{14}$) with ellipsoids at 50% probability. Hydrogen atoms, lattice solvent, and the $GaCl_4$ counteranions are omitted for clarity. Selected bond lengths [Å] and angles [°]: Au(1)···B(1), 3.121(3); Au(1)–P(1), 2.3149(6); Au(1)–P(2), 2.3178(7); P(1)–Au(1)–P(2), 158.84(2); C(28)–B(1)–C(33), 117.8(2); C(28)–B(1)–C(39), 120.8(2); C(33)–B(1)–C(39), 120.8(2).

SUMMARY AND CONCLUSIONS

UV Photolysis of a solution of FcPPB and $[W(CO)_6]$ provided $[W(CO)_4(\kappa^2PP\text{-FcPPB*})]$ (**1**), where the FcPPB* ligand is the result of intramolecular electrophilic attack of the borane on the proximal cyclopentadienyl ring, followed by loss of a cyclopentadienyl hydrogen atom and a *B*-phenyl ring as benzene. Metallocene borylation reactivity is typically associated with more electrophilic boranes, and to the best of our knowledge, the reaction to form **1** is the first example involving a non-fluorinated

tris(hydrocarbyl)borane. FcPPB and $[W(CO)_6]$ did not react under thermal conditions (80 °C for days). Furthermore, FcPPB is unreactive under photochemical conditions, and we hypothesized that this may be due to intramolecular phosphine-borane adduct formation, which prevents the borane from interacting with the adjacent cyclopentadienyl ring.

In an effort to disrupt the intramolecular $C_5H_4(^tBu)(Ar)P\rightarrow BPh_2Ar$ interaction in the free ligand, FcPPB was reacted with $B(C_6F_5)_3$ and $BF_3(OEt_2)$. However, $B(C_6F_5)_3$ afforded a 1:1 adduct (**2**) in which the original intramolecular phosphine–borane interaction is maintained, and $BF_3(OEt_2)$ yielded a boronium cation (**3**) resulting from loss of a phenyl anion from the borane unit in FcPPB. The differing reactivity of $BF_3(OEt_2)$ and $B(C_6F_5)_3$ suggests that the B–F linkages in $BF_3(OEt_2)$ are intimately involved in the reaction pathway leading to phenyl anion loss from the borane in FcPPB.

By contrast, reaction of FcPPB with $[Au(PPh_3)][GaCl_4]$ afforded dimetallic $[\{Au(FcPPB)\}_2][GaCl_4]_2$ (**4**) as a mixture of diastereomers with μ-1κ*P*:2κ*P'*-coordinated FcPPB ligands. Compound **4** extends the reported series of borane-appended gold complexes, and exhibits the longest Au–B distance with the least pyramidalization at boron. These features, combined with a high-frequency ^{11}B NMR chemical shift (68 ppm), are indicative of little or no Au–B interaction, likely due to the combined effect of (a) cationic gold centres with low nucleophilicity, and (b) the donor–donor–acceptor array of FcPPB, which permits a greater range of Au···B distances relative to ambiphilic ligands in which the borane is flanked by two or more phosphine donors. Nevertheless, **4** proved unreactive under UV photolysis conditions, suggesting that ferrocene borylation may not be a general feature of the chemistry of FcPPB, even when the borane is weakly- or non-coordinated.

EXPERIMENTAL SECTION

An argon-filled MBraun UNIlab glove box equipped with a −30 °C freezer was employed for the manipulation and storage of the FcPPB ligand and its complexes, and reactions were performed on a double manifold high vacuum line using standard techniques.[41] A Fisher Scientific Ultrasonic FS-30 bath was used to sonicate reaction mixtures where indicated. Residual oxygen and moisture was removed from the argon stream by passage through an Oxisorb-W scrubber from Matheson Gas Products.

Hexanes and benzene were initially dried and distilled at atmospheric pressure from Na/Ph_2CO, and toluene was initially dried and distilled at atmospheric pressure from Na. Unless otherwise noted, all protio solvents were stored over an appropriate drying agent (toluene, benzene = Na/Ph_2CO; hexanes = Na/Ph_2CO/tetraglyme) and introduced to reactions via vacuum transfer with condensation at −78 °C. Deuterated solvents (ACP Chemicals) were dried over Na/Ph_2CO (C_6D_6) of CaH_2 (CD_2Cl_2).

1,1'-Bisdiphenylphosphinoferrocene (dppf), $[W(CO)_6]$, $GaCl_3$, $BF_3(OEt_2)$, BPh_3, BEt_3, and $AlMe_3$ were purchased from Sigma-Aldrich and either used as is or stored under argon. C_6F_5Br {used for the synthesis of $B(C_6F_5)_3$} was purchased from Oakwood Chemicals and distilled from molecular sieves prior to use. Argon of 99.999 % purity was purchased from Praxair. FcPPB was prepared according to the literature procedure.[4] $B(C_6F_5)_3$ was prepared from C_6F_5MgBr and $BF_3{\cdot}Et_2O$ according to the literature procedure.[42] $[W(CO)_4(dppf)]$ was prepared according to the literature procedure.[43]

The purity of all new complexes was evaluated by solution NMR spectroscopy (^1H, ^{13}C, ^{31}P, ^{11}B, and in some cases also ^{19}F NMR) as well as combustion elemental analysis (EA). Acceptable EAs were obtained for compounds **1** and **4**. However, as noted in the individual experimental sections, the elemental analyses for **2** and **3** are not within the expected range; this deviation is thought to be due to problems with the accuracy of the analysis during the period of time in which these samples were available, and not due to the presence of significant impurities, since NMR spectra show that **2** and **3** were isolated in reasonable purity (a PXRD of **3** also indicates that the bulk sample corresponds to that of the single crystal X-ray crystal structure), the samples dissolved entirely for NMR (i.e. no solid residue remained), and the reactions to form **2** and **3** are not likely to generate NMR-silent impurities (such as a metal halide).

IR Spectra were recorded on a Thermo Scientific Nicolet 6700 FTIR spectrometer (reported stretches are strong unless otherwise noted). Combustion elemental analyses were performed on a Thermo EA1112 CHNS/O analyzer. A VWR Clinical 200 Large Capacity Centrifuge (with 28° fixed-angle rotors that hold 12 × 15 mL or 6 × 50 mL tubes) in combination with VWR high-performance polypropylene conical centrifuge tubes was used when required (inside the glovebox). A 0.75×1.5×0.5 meter UV cabinet equipped with a 4×25 watt (18") Sylvania Ecologic 350 blacklight bulbs (model: F25T8/350BL/ECO; peak output 356 nm; output from ~310-400 nm), in conjunction with quartz J-Young NMR tubes and quartz 125 mL single-necked round bottom flasks were utilized for the synthesis of **1**.

NMR spectroscopy (^1H, $^{13}C\{^1H\}$, $^{31}P\{^1H\}$, ^{19}F, ^{11}B, ^{13}C-DEPT-135, ^{13}C-uDEFT, ^1H-^1H-COSY, ^1H-^{13}C-HSQC, ^1H-^{13}C-HMBC, ^1H-^{31}P-HMBC) was performed on Bruker AV-200, DRX-500 and AV-600 spectrometers. All ^1H NMR and $^{13}C\{^1H\}$ NMR spectra were referenced relative to $SiMe_4$ through a resonance of the employed deuterated solvent or protio impurity of the solvent; C_6D_6 (7.16 ppm) and CD_2Cl_2 (5.32 ppm) for ^1H NMR; C_6D_6 (128.0 ppm) and CD_2Cl_2 (54.00 ppm) for $^{13}C\{^1H\}$ NMR. $^{31}P\{^1H\}$, ^{19}F and ^{11}B NMR spectra were referenced using an external standard of 85% H_3PO_4 in D_2O (0.0 ppm), $CFCl_3$ (0.0 ppm) and $BF_3(OEt_2)$ (0.0 ppm), respectively. Temperature calibration was performed using a d_4-methanol sample, as outlined in the Bruker VTU user manual.

Herein, numbered proton and carbon atoms refer to the positions of the C_5H_4 rings and the phenylene linker within the FcPPB ligand backbone. The C_5H_4 ring bound to the $C_5H_4P(^tBu)Ar$ phosphine was numbered $C^{1'\text{-}5'}$, where $C^{1'}$ is the *ipso*-carbon atom bound to phosphorus, and the C_5H_4 ring bound to the $C_5H_4PPh_2$ phosphine was numbered $C^{1''\text{-}5''}$, where $C^{1''}$ is the *ipso*-carbon atom bound to phosphorus. The phenylene linker is numbered such that C^1 refers to the carbon atom bound to the phosphine moiety, and C^2 refers to the carbon atom bound to the borane. The remainder of the carbon atoms and protons in the phenylene linker were numbered accordingly in both cases. Inequivalent phenyl rings on phosphorus and boron are labelled A and B so that the proton and carbon resonances belonging to a single phenyl ring can be identified. We did not identify which *P*- or *B*-phenyl rings give rise to the signals labelled A or B, respectively.

Single crystal X-ray diffraction analyses were performed on suitable crystals coated in Paratone oil and mounted on a SMART APEX II diffractometer with a 3 kW Sealed tube Mo generator in the McMaster Analytical X-Ray (MAX) Diffraction Facility. In all cases, non-hydrogen atoms were refined anisotropically and hydrogen atoms were generated in ideal positions and then updated with each cycle of refinement. One molecule of benzene in $[W(CO)_4(FcPPB^*)]{\cdot}C_6H_6$ was disordered over two positions in 72:28 ratio; both orientations were restrained to a hexagon via the AFIX 66 command, and the thermal ellipsoids of both orientations were refined to have similar thermal parameters through the use of the SIMU command. In addition, $[FcPPB^{-Ph}][BF_4]$ crystallized as a racemic twin in a 55:45 ratio. The 2D powder X-ray diffraction experiment was performed on a Bruker SMART6000 CCD diffractometer with a Rigaku RU200 Cu rotating anode source ($\lambda = 0.154$ nm) operated at 50 kV and 90 mA. Powdered **3** was packed in 0.5 mm o.d. special glass (SG; wall thickness 0.01 mm) capillary tube for X-ray diffraction (purchased from Charles Supper Co.) and sealed by inverting to submerge the open end in a pool of Apiezon H-grease within the glovebox. The calculated powder pattern for **3** was generated from the low-temperature single crystal data using Mercury. The experimental powder diffractogram was generated and viewed using Gadds, Powdercell, Crystal Sleuth, and Topas.

[W(CO)$_4$(FcPPB*)] (1): A toluene solution (15 mL) of FcPPB (199 mg, 0.285 mmol) and [W(CO)$_6$] (100 mg, 0.285 mmol) in a 125 mL quartz flask equipped with a glass Schlenk adapter was irradiated under UV-A radiation for 24 hours under a static atmosphere of argon (max pressure increase from CO evolution ~15%). The bright orange solution was evaporated to dryness *in vacuo* and the resulting orange solid was brought into the glovebox, washed with cold hexanes (~10 mL) and dried *in vacuo*. Yield = 214 mg (82%). X-ray quality crystals were grown by slow diffusion of hexanes into a solution of **1** in benzene at room temperature. **^{1}H NMR (600 MHz, CD$_2$Cl$_2$, 298 K):** δ 8.17 (dd, $^3J_{H,P}$ 13 Hz, $^3J_{H,H}$ 8 Hz, 1H, C*H*^{6}), 8.02 (dt, $^3J_{H,H}$ 7 Hz, $^4J_{H,P}$ 1 Hz, 1H, C*H*^{3}), 7.74–7.71 (m, 2H, *o*-P*Ph*$_2$ A), 7.67–7.66 (m, 3H, C*H*^{5}, *o*-B*Ph*), 7.51 (tt, $^3J_{H,H}$ 7 Hz, $^3J_{H,H}$ 1 Hz, 1H, C*H*^{4}), 7.49–7.47 (m, 6H, *m*,*p*-P*Ph*$_2$ A, *m*,*p*-B*Ph*), 7.25–7.23 (m, 1H, *p*-P*Ph*$_2$ B), 7.22–7.18 (m, 4H, *o*,*m*-P*Ph*$_2$ B), 5.42 (s, 1H, C*H*$^{5'}$), 4.94 (s, 1H, C*H*$^{4'}$), 4.50 (s, 1H, C*H*$^{3'}$), 4.45 (s, 1H, C*H*$^{5''/2''}$), 4.23 (s, 1H, C*H*$^{3''/4''}$), 3.99 (s, 1H, C*H*$^{4''/3''}$), 3.66 (s, 1H, C*H*$^{2''/5''}$), 1.07 (d, $^3J_{H,P}$ 14 Hz, 9H, C*Me*$_3$). **^{13}C{^{1}H} NMR (151 MHz, CD$_2$Cl$_2$, 298 K):** δ 208.4 (dd, $^2J_{C,P}$ 26 Hz, $^2J_{C,P}$ 6 Hz, W-*C*O), 205.8 (appt. t, $^2J_{C,P}$ 7 Hz, W-*C*O), 204.8 (dd, $^2J_{C,P}$ 24 Hz, $^2J_{C,P}$ 5 Hz, W-*C*O), 203.0 (appt. t, $^2J_{C,P}$ 7 Hz, W-*C*O), 143.1 (broad s, *ipso*-B*Ph*), 142.0 (d, $^1J_{C,P}$ 31 Hz, *C*^{1}), 140.6 (broad s, *C*^{2}), 140.3 (d, $^3J_{C,P}$ 6 Hz, *C*^{3}), 139.9 (d, $^1J_{C,P}$ 42 Hz, *ipso*-P*Ph*$_2$ B), 137.7 (d, $^2J_{C,P}$ 25 Hz, *C*^{6}), 136.2 (d, $^1J_{C,P}$ 39 Hz, *ipso*-P*Ph*$_2$ A), 134.4 (d, $^2J_{C,P}$ 13 Hz, *o*-P*Ph*$_2$ A), 133.7 (s, *o*-B*Ph*), 132.8 (d, $^2J_{C,P}$ 11 Hz, *o*-P*Ph*$_2$ B), 130.9 (s, *C*^{5}), 130.8 (s, *p*-P*Ph*$_2$ A), 129.8 (s, *p*-P*Ph*$_2$ B), 129.7 (s, *C*^{4}), 129.4 (s, *p*-B*Ph*), 128.8 (d, $^3J_{C,P}$ 10 Hz, *m*-P*Ph*$_2$ A), 128.2 (d, $^3J_{C,P}$ 9 Hz, *m*-P*Ph*$_2$ B), 128.1 (s, *m*-B*Ph*), 86.1 (d, $^2J_{C,P}$ 19 Hz, *C*$^{5'}$), 84.5 (dd, $^1J_{C,P}$ 38 Hz, $^3J_{C,P}$ 3 Hz, *C*$^{1'}$), 83.8 (d, $^1J_{C,P}$ 38 Hz, *C*$^{1''}$), 80.0 (d, $^3J_{C,P}$ 8 Hz, *C*$^{4'}$), 79.8 (s, *C*$^{3'}$), 78.6 (d, $^2J_{C,P}$ 18 Hz, *C*$^{2''/5''}$), 75.1 (d, $^2J_{C,P}$ 7 Hz, *C*$^{5''/2''}$), 73.4 (s, *C*$^{4''/3''}$), 72.9 (d, $^3J_{C,P}$ 3 Hz, *C*$^{3''/4''}$), 38.3 (d, $^1J_{C,P}$ 21 Hz, *C*Me$_3$), 27.7 (d, $^2J_{C,P}$ 5 Hz, C*Me*$_3$); *C*$^{2'}$ could not be located. **^{31}P{^{1}H} (203 MHz, CD$_2$Cl$_2$, 298 K):** δ 19.7 (d, $^1J_{P,W}$ 233 Hz, $^2J_{P,P}$ 24 Hz, C$_5$H$_4$*P*(^{t}Bu)Ar), 14.2 (d, $^1J_{P,W}$ 236 Hz, $^2J_{P,P}$ 24 Hz, C$_5$H$_4$*P*Ph$_2$). **^{11}B NMR (161 MHz, CD$_2$Cl$_2$, 298 K):** δ 57 (broad s, ω$_{1/2}$ = 1200 Hz). **IR (nujol):** ν(CO) = 2014, 1907, 1889, 1851, 1846 cm^{-1}. **IR (CH$_2$Cl$_2$):** 2015, 1934, 1910, 1892, 1868 cm^{-1}. **Anal. Calcd.** For C$_{42}$H$_{35}$BFeO$_4$P$_2$W: C, 55.06; H, 3.85%. **Found:** C, 55.22; H, 4.24%.

FcPPB{B(C$_6$F$_5$)$_3$} (2): Benzene (10 mL) was condensed into a 50 mL round bottom flask containing FcPPB (75.9 mg, 0.114 mmol) and B(C$_6$F$_5$)$_3$ (55.6 mg, 0.114 mmol) through the use of a dry ice/acetone bath, and the reaction mixture was stirred overnight at room temperature. The reaction solution was then evaporated to dryness *in vacuo* to yield an orange solid. Yield = 95.0 mg (69 %). Despite numerous attempts, a satisfactory elemental analysis was not obtained for **2**. However, the NMR spectra presented in the supporting information indicate the **2** was isolated in reasonable purity. **^{1}H NMR (600 MHz, C$_6$D$_6$, 298 K):** 7.94 (broad s, 2H, *o*-B*Ph*$_2$ A), 7.88 (broad s, 2H, *o*-B*Ph*$_2$ B), 7.68–7.66 (m, 3H, C*H*^{3}, *o*-P*Ph*$_2$ A), 7.48 (broad s, 2H, *m*-B*Ph*$_2$ A), 7.42–7.38 (m, 2H, C*H*^{4}, *p*-B*Ph*$_2$ A), 7.29 (t, $^3J_{H,H}$ 9 Hz, 2H, *o*-P*Ph*$_2$ B), 7.26 (broad s, 2H, *m*-B*Ph*$_2$ B), 7.16 (app. s, 2H, C*H*^{5}, *p*-B*Ph*$_2$ B), 7.11 (t, $^3J_{H,H}$ 7 Hz, 1H, C*H*^{6}), 7.05 (t, $^3J_{H,H}$ 7 Hz, 1H, *p*-P*Ph*$_2$ A), 7.00 (t, $^3J_{H,H}$ 7 Hz, 1H, *p*-P*Ph*$_2$ B), 6.95 (td, $^3J_{H,H}$ 7 Hz, $^4J_{H,P}$ 2 Hz, 2H, *m*-P*Ph*$_2$ A), 6.80 (td, $^3J_{H,H}$ 8 Hz, $^4J_{H,P}$ 2 Hz, 2H, *m*-P*Ph*$_2$ B), 4.29 (s, 1H, C*H*$^{2'/5'}$), 3.78 (s, 1H, C*H*$^{5'/2'}$), 3.69 (s, 1H, C*H*$^{3'/4'}$), 3.56 (s, 1H, C*H*$^{4'/3'}$), 3.40 (s, 1H, C*H*$^{3''/4''}$), 3.29 (s, 1H, C*H*$^{2''/5''}$), 3.25 (s, 1H, C*H*$^{4''/3''}$), 2.97 (s, 1H, C*H*$^{5''/2''}$), 0.69 (d, $^3J_{H,P}$ 14 Hz, 9H, C*Me*$_3$). **^{13}C{^{1}H} NMR (151 MHz, C$_6$D$_6$, 298 K:** 163.9 (broad d, $^2J_{C,P}$ 42 Hz, *C*^{2}), 148.8 (d, $^1J_{C,F}$ 241 Hz, *o*-B(*C*$_6$F$_5$)$_3$), 146.8 (broad s, *ipso*-B*Ph*$_2$ A and B), 140.7 (broad d, $^1J_{C,F}$ 253 Hz, *p*-B(*C*$_6$F$_5$)$_3$), 137.4 (ddd, $^1J_{C,F}$ 248 Hz, $^2J_{C,F}$ 19 Hz, $^4J_{C,P}$ 12 Hz, *m*-B(*C*$_6$F$_5$)$_3$), 135.3 (s, *o*-B*Ph*$_2$ B), 134.4 (d, $^2J_{C,P}$ 9 Hz, *o*-P*Ph*$_2$ A), 133.9 (d, $^2J_{C,P}$ 9 Hz, *o*-P*Ph*$_2$ B, *o*-B*Ph*$_2$ A), 132.1 (s, *C*^{4}), 131.7 (s, *C*^{3}), 131.7 (s, *p*-P*Ph*$_2$ B), 131.5 (s, *p*-P*Ph*$_2$ A), 129.5 (s, *C*^{6}), 128.4 (s, *p*-B*Ph*$_2$ B), 128.2 (d, $^3J_{C,P}$ 10 Hz, *m*-P*Ph*$_2$ B), 127.9 (d, $^3J_{C,P}$ 10 Hz, *m*-P*Ph*$_2$ A), 127.9 (s, *m*-B*Ph*$_2$ A+B), 127.7 (s, *p*-B*Ph*$_2$ A), 127.6 (d, $^3J_{C,P}$ 6 Hz, *C*^{5}), 116.1 (broad s, *ipso*-B(C$_6$F$_5$)$_3$), 77.1 (d, $^2J_{C,P}$ 19 Hz, *C*$^{2'/5'}$), 76.8 (d, $^3J_{C,P}$ 5 Hz, *C*$^{4''/3''}$), 75.5 (d, $^2J_{C,P}$ 12 Hz, *C*$^{2''/5''}$), 75.1 (dd, $^1J_{C,P}$ 118 Hz, $^3J_{C,P}$ 11 Hz, *C*$^{1'/1''}$), 75.0 (d, $^2J_{C,P}$ 10 Hz, *C*$^{5''/2''}$), 74.0 (d, $^3J_{C,P}$ 7 Hz, *C*$^{3'/4'}$), 73.1 (d, $^2J_{C,P}$ 3 Hz, *C*$^{5'/2'}$), 72.5 (d, $^3J_{C,P}$ 7 Hz, *C*$^{3''/4''}$), 72.0 (s, *C*$^{4'/3'}$), 71.5 (dd, $^1J_{C,P}$ 53 Hz, $^3J_{C,P}$ 8 Hz, *C*$^{1'/1''}$), 34.1 (d, $^1J_{C,P}$ 3 Hz, *C*Me$_3$), 27.4 (d, $^2J_{C,P}$ 5 Hz, C*Me*$_3$). **^{19}F NMR (188 MHz, C$_6$D$_6$, 298 K):** δ –125.1 (s, *o*-B(C$_6$F$_5$)$_3$), –156.7 (s, *p*-B(C$_6$F$_5$)$_3$), –164.3 (s, *m*-B(C$_6$F$_5$)$_3$). **^{31}P{^{1}H} NMR (203 MHz, C$_6$D$_6$, 298 K):** δ 20.0 (broad s, ω$_{1/2}$ 93 Hz, C$_5$H$_4$*P*Ph$_2$), 15.1 (s, C$_5$H$_4$*P*(^{t}Bu)Ar). **^{11}B NMR (161 MHz, C$_6$D$_6$, 298 K):** δ 25 (broad s, ω$_{1/2}$ 2300 Hz, Ar*B*Ph$_2$), –4 (broad s, ω$_{1/2}$ 1200 Hz, *B*(C$_6$F$_5$)$_3$). **Anal. Calcd.** For C$_{62}$H$_{41}$B$_2$F$_{15}$FeP$_2$: C, 61.52; H, 3.41%. **Found:** C, 62.52; H, 5.07%.

[FcPPB$^{–Ph}$][BF$_4$] (3): Benzene (15 mL) was condensed into a 50 mL Schlenk flask containing FcPPB (108 mg, 0.155 mmol) and BF$_3$(OEt$_2$) (22.0 mg, 0.155 mmol) through the use of a dry ice/acetone bath. The reaction solution was stirred for 3 days at 70 °C, after which point the precipitated pale orange solid was isolated by centrifugation and dried *in vacuo*. Yield = 69.9 mg (64 %). Despite numerous attempts, a satisfactory elemental analysis was not obtained for **3**. However, the NMR spectra and powder X-ray diffractogram presented in the supporting information indicate the **3** was isolated in reasonable purity. X-ray quality crystals precipitated from a solution of FcPPB (14.8 mg, 2.12×10^{-2} mmol) and BF$_3$(OEt$_2$) (6.00 mg, 2.12×10^{-2} mmol) in benzene at room temperature. **^{1}H NMR (600 MHz, CD$_2$Cl$_2$, 298 K):** δ 7.86–7.83 (m, 1H, *p*-P*Ph*$_2$ A), 7.80 (t, $^3J_{H,H}$ 9 Hz, 1H, C*H*^{3}), 7.77–7.71 (m, 5H, C*H*^{4}, *o*,*m*-P*Ph*$_2$ A), 7.68–7.65 (m, 2H, C*H*^{5}, *p*-P*Ph*$_2$ B), 7.41 (dt, $^3J_{H,H}$ 8 Hz, $^4J_{H,P}$ 3 Hz, 4H, *m*-P*Ph*$_2$ B, *o*-B*Ph*), 7.29 (tp, $^3J_{H,H}$ 7 Hz, $^4J_{H,H}$ 2 Hz, 1H, *p*-B*Ph*), 7.23 (t, $^3J_{H,H}$ 7 Hz, 2H, *m*-B*Ph*), 7.03 (ddd, $^3J_{H,P}$ 12 Hz, $^3J_{H,H}$ 8 Hz, $^4J_{H,H}$ 1 Hz, 2H, *o*-P*Ph*$_2$ B), 6.76 (d, $^3J_{H,H}$ 8 Hz, 1H, C*H*^{6}), 5.03 (sextet, $^3J_{H,H}$ 1 Hz, 1H, C*H*$^{2'/5'}$), 4.83 (septet, $^3J_{H,H}$ 1 Hz, 1H, C*H*$^{3'/4'}$), 4.72 (dt, $^3J_{H,H}$ 3 Hz, $^4J_{H,H}$ 1 Hz, 1H, C*H*$^{4'/3'}$), 4.63 (septet, $^3J_{H,H}$ 1 Hz, 1H, C*H*$^{4''/3''}$), 4.60 (septet, $^3J_{H,H}$ 1 Hz, 1H, C*H*$^{5'/2'}$), 4.57 (septet, $^3J_{H,H}$ 1 Hz, 1H, C*H*$^{3''/4''}$), 3.69 (septet, $^3J_{H,H}$ 1 Hz, 1H, C*H*$^{2''/5''}$), 3.17 (s, 1H, C*H*$^{5''/2''}$), 1.12 (d, $^3J_{H,P}$ 16 Hz, 9H, C*Me*$_3$). **^{13}C NMR (151 MHz, CD$_2$Cl$_2$, 298 K):** δ 155.5 (broad s, *C*^{2}), 135.8 (t, $^3J_{C,P}$ 6 Hz, *o*-B*Ph*), 135.4 (s, *C*^{5}), 134.8 (d, $^2J_{C,P}$ 10 Hz, *o*-P*Ph*$_2$ A), 134.5 (s, *p*-P*Ph*$_2$ A), 134.1 (d, $^2J_{C,P}$ 9 Hz, *o*-P*Ph*$_2$ B), 133.9 (s, *p*-P*Ph*$_2$ B), 133.5 (dd, $^1J_{C,P}$ 61 Hz, $^3J_{C,P}$ 13 Hz, *C*^{1}), 132.9 (d, $^2J_{C,P}$ 31 Hz, *C*^{6}), 131.9 (d, $^4J_{C,P}$ 8 Hz, *C*^{4}), 130.4 (d, $^3J_{C,P}$ 11 Hz, *m*-P*Ph*$_2$ A), 129.9 (s, *C*^{3}), 129.8 (d, $^3J_{C,P}$ 11 Hz, *m*-P*Ph*$_2$ B), 129.0 (s, *m*-B*Ph*), 129.0 (s, *p*-B*Ph*), 123.1 (d, $^1J_{C,P}$ 64 Hz, *ipso*-P*Ph*$_2$ A), 122.3 (dd, $^1J_{C,P}$ 64 Hz, $^3J_{C,P}$ 9 Hz, *ipso*-P*Ph*$_2$ B), 78.7 (s, *C*$^{5'/2'}$), 77.4 (appt t, $J_{C,P}$ 8 Hz, *C*$^{3'/4'}$, *C*$^{2''/5''}$), 77.0 (d, $^3J_{C,P}$ 8 Hz, *C*$^{4''/3''}$), 75.0 (d, $^2J_{C,P}$ 15 Hz, *C*$^{2'/5'}$), 74.7 (d, $^3J_{C,P}$ 6 Hz, *C*$^{4'/3'}$), 74.6 (d, $^2J_{C,P}$ 11 Hz, *C*$^{5''/2''}$), 74.4 (d, $^3J_{C,P}$ 8 Hz, *C*$^{3''/4''}$), 65.0 (d, $^1J_{C,P}$ 76 Hz, *C*$^{1''}$), 62.7 (d, $^1J_{C,P}$ 43 Hz, *C*$^{1'}$), 36.1 (d, $^1J_{C,P}$ 16 Hz, *C*Me$_3$), 26.1 (s, C*Me*$_3$). **^{19}F NMR (188 MHz, CD$_2$Cl$_2$, 298 K):** δ –152.9 (s, B*F*$_4$). **^{31}P{^{1}H} NMR (203 MHz, CD$_2$Cl$_2$, 298 K):** δ 27.8 (broad s, ω$_{1/2}$ 65 Hz, C$_5$H$_4$*P*(^{t}Bu)Ar), 1.0 (broad s, ω$_{1/2}$ 150 Hz, C$_5$H$_4$*P*Ph$_2$). **^{11}B NMR (161 MHz, CD$_2$Cl$_2$, 298 K):** δ –1.4 (s, *B*F$_4$), –2.0 (broad s, ω$_{1/2}$ 250 Hz, FcPP*B*^{Ph}). **Anal. Calcd.** For C$_{38}$H$_{36}$B$_2$F$_4$FeP$_2$: C, 64.45; H, 5.13%. **Found:** C, 62.52; H, 5.07%.

[{Au(FcPPB)}$_2$][GaCl$_4$]$_2$ (4): Toluene (30 mL) was condensed into a 100 mL round bottom flask containing [AuCl(PPh$_3$)] (177 mg, 0.358 mmol) and GaCl$_3$ (63.0 mg, 0.358 mmol) through the use of a dry ice/acetone bath. The reaction mixture was stirred for 1 hour at room temperature, at which point a solution of FcPPB (250 mg, 0.358 mmol) in toluene (10 mL) was added; the resulting reaction mixture was stirred overnight at room temperature. After stirring overnight a dark orange oil had precipitated from solution; the solvent was removed *in vacuo* and hexanes (~30 mL) were added to the crude material. The hexanes slurry was sonicated for 15 minutes, resulting in the precipitation of a tangerine solid, which was then filtered through the use of a swivel frit. The collected tangerine solid was washed with hexanes (2 × 10 mL) and dried *in vacuo*. Yield = 355 mg (90 %). [{Au(FcPPB)}$_2$][GaCl$_4$]$_2$ was isolated as a diastereomeric mixture in a 65:35 ratio; the NMR signals corresponding to the diastereomer of highest concentration are denoted as "A". X-ray quality crystals of *meso*-[{Au(FcPPB)}$_2$][GaCl$_4$]$_2$·2(C$_6$H$_{14}$) were obtained by slow diffusion of hexanes into a solution of [{Au(FcPPB)}$_2$][GaCl$_4$]$_2$ in CH$_2$Cl$_2$ at –30 °C. **^{1}H NMR (CD$_2$Cl$_2$, 600 MHz, 298 K):** δ 8.06–7.99 (m, aryl-C*H*), 7.90 (t, *J* 7 Hz, aryl-C*H*), 7.86–7.71 (m, aryl-C*H*), 7.69–7.54 (m, aryl-C*H*), 7.45 (dt, *J* 8 Hz, *J* 2 Hz, aryl-C*H*), 7.41 (t, *J* 7 Hz, aryl-C*H*), 7.34–7.28 (m, aryl-C*H*), 7.22 (t, *J* 8 Hz, aryl-C*H*), 7.13 (t, *J* 8 Hz, aryl-C*H*), 6.96–6.88 (m, aryl-C*H*), 6.83 (d, *J* 7 Hz, aryl-C*H*), 6.61 (dd, *J* 13 Hz, *J* 8 Hz, aryl-C*H*), 5.31 (s, 1H, C*H*$^{2'/5'}$ B), 5.05 (s, 1H, C*H*$^{5'/2'}$ B), 5.00 (s, 4H, C*H*$^{2'/5'}$ A, C*H*$^{5'/2'}$ A), 4.71 (s, 2H, C*H*$^{2''/5''}$ A), 4.63 (s, 2H, C*H*$^{2''/5''}$ B, C*H*$^{4''/3''}$ B), 4.60 (s, 2H, C*H*$^{5''/2''}$ A), 4.52 (s, 1H, C*H*$^{3'/4'}$ B), 4.44 (s, 2H, C*H*$^{4''/3''}$ A), 4.20 (s, 1H, C*H*$^{4'/3'}$ B), 4.17 (s, 2H, C*H*$^{3'/4'}$ A), 3.99 (s, 2H, C*H*$^{3''/4''}$ A), 3.96 (s, 1H, C*H*$^{5''/2''}$ B), 3.76 (s, 1H, C*H*$^{3''/4''}$ B), 3.66 (s,

2H, C*H*$^{4'/3'}$ A), 0.94 (d, $^{3}J_{H,P}$ 18 Hz, 18H, C*Me*$_3$ A), 0.75 (d, $^{3}J_{H,P}$ 18 Hz, 9H, C*Me*$_3$ B). **^{13}C{^{1}H} NMR (CD_2Cl_2, 151 MHz, 298 K):** δ 155.2 (d, *J* 32 Hz, aryl-*C* A), 154.8 (d, *J* 31 Hz, aryl-*C* B), 143.2, 142.5, 142.4, 140.4, 140.0, 139.4, 138.3, 136.4, 135.9, 134.4, 134.3, 133.9, 133.4, 133.2, 132.9, 132.4, 132.2, 132.0, 131.4, 131.2, 131.1, 131.0, 130.2, 129.4, 128.9, 128.7 (26 × s, aryl-*C*), 135.5 (d, *J* 14 Hz, aryl-*C*), 134.6–134.4 (m, aryl-*C*), 132.6 (d, *J* 13 Hz, aryl-*C*), 131.0 (d, *J* 7 Hz, aryl-*C*), 130.7 (d, *J* 12 Hz, aryl-*C*), 130.6 (d, *J* 12 Hz, aryl-*C*), 130.4 (d, *J* 7 Hz, aryl-*C*), 130.1 (d, *J* 12 Hz, aryl-*C*), 129.9 (d, *J* 11 Hz, aryl-*C*), 129.5 (d, *J* 8 Hz, aryl-*C*), 126.6 (dd, *J* 57 Hz, *J* 4 Hz, aryl-*C*), 80.1 (d, $^{2}J_{C,P}$ 25 Hz, *C*$^{2'/5'}$ B), 80.0 (d, $^{2}J_{C,P}$ 24 Hz, *C*$^{2'/5'}$ A), 78.5 (d, $^{2}J_{C,P}$ 26 Hz, *C*$^{2''/5''}$ A), 77.1 (d, $^{3}J_{C,P}$ 7 Hz, *C*$^{4''/3''}$ A), 77.0 (d, $^{3}J_{C,P}$ 10 Hz, *C*$^{3''/4''}$ B), 76.4 (s, *C*$^{5''/2''}$ B), 75.8 (s, *C*$^{5'/2'}$ A), 75.6 (d, $^{3}J_{C,P}$ 7 Hz, *C*$^{4'/3'}$ B), 75.5 (d, $^{3}J_{C,P}$ 7 Hz, *C*$^{4''/3''}$ B), 75.4 (d, $^{3}J_{C,P}$ 5 Hz, *C*$^{4'/3'}$ A), 75.3 (s, *C*$^{5''/2''}$ A), 74.8 (s, *C*$^{5'/2'}$ B), 74.7 (s, *C*$^{3'/4'}$ B), 74.0 (d, $^{2}J_{C,P}$ 11 Hz, *C*$^{2''/5''}$ B), 73.9 (s, *C*$^{3'/4'}$ A), 72.6 (d, $^{3}J_{C,P}$ 11 Hz, *C*$^{3''/4''}$ A), 72.1 (d, $^{1}J_{C,P}$ 63 Hz, *C*$^{1'/1''}$ A/B), 70.3 (d, $^{1}J_{C,P}$ 65 Hz, *C*$^{1'/1''}$A/B), 38.5 (d, $^{1}J_{C,P}$ 29 Hz, *C*Me$_3$ A), 38.4 (d, $^{1}J_{C,P}$ 31 Hz, *C*Me$_3$ B), 28.5 (d, $^{2}J_{C,P}$ 6 Hz, C*Me*$_3$ A), 28.4 (d, $^{2}J_{C,P}$ 6 Hz, C*Me*$_3$ B). **^{31}P{^{1}H} NMR (CD_2Cl_2, 203 MHz, 298 K):** δ 63.3 (d, $^{2}J_{P,P}$ 310 Hz, C_5H_4P(^{t}Bu)Ar B), 63.1 (d, $^{2}J_{P,P}$ 302 Hz, C_5H_4P(^{t}Bu)Ar A), 40.7 (d, $^{2}J_{P,P}$ 310 Hz, $C_5H_4PPh_2$ B), 39.1 (d, $^{2}J_{P,P}$ 302 Hz, $C_5H_4PPh_2$ A). **^{11}B NMR (CD_2Cl_2, 161 MHz, 298 K):** δ 68 (broad s, $\omega_{1/2}$ 3000 Hz). **Elemental Analysis Calcd (%)** for $C_{44}H_{41}AuBCl_4FeGaP_2$: C, 47.74; H, 3.73%. **Found:** C, 47.45; H, 3.94%.

ASSOCIATED CONTENT

Supporting Information

NMR spectra for compounds **1**–**4**, PXRD of **3**, and X-ray structure refinement details for **1**·C_6H_6, **3**, and *meso*-**4**·$2C_6H_{14}$ is included in the Supporting Information, which is available free of charge on the ACS Publications website. CCDC 1816559-1816561 contain the supplementary crystallographic data for **1**·C_6H_6, *meso*-**4**·$2C_6H_{14}$, and **3**, respectively. These data can be obtained free of charge from The Cambridge Crystallographic Data Centre via www.ccdc.cam.ac.uk/data_request/cif.

AUTHOR INFORMATION

Corresponding Author

* Phone: (905) 527-9140, Fax: (905) 522-2509. E-mail: emslied@mcmaster.ca.

ORCID

David J. H. Emslie: 0000-0002-2570-9345

Notes

The authors declare no competing financial interest.

ACKNOWLEDGMENT

D.J.H.E. thanks NSERC of Canada for a Discovery Grant and B.E.C. thanks the Government of Canada for an NSERC PGS-D scholarship. We are grateful to J. S. Price for PXRD on **3** (Figure S33), and to R. Chadwick in the Adronov Lab at McMaster University for assistance with, and access to, a UV cabinet.

REFERENCES

(1) Hill, A. F.; Owen, G. R.; White, A. J. P.; Williams, D. J. The Sting of the Scorpion: A Metallaboratrane, *Angew. Chem. Int. Ed.* **1999**, *38*, 2759-2761.

(2) (a) Bouhadir, G.; Amgoune, A.; Bourissou, D. Phosphine-Boranes and Related Ambiphilic Compounds: Synthesis, Structure, and Coordination to Transition Metals, *Adv. Organomet. Chem.* **2010**, *58*, 1-107. (b) Fontaine, F.-G.; Boudreau, J.; Thibault, M. H. Coordination Chemistry of Neutral (L_n)-Z Amphoteric and Ambiphilic Ligands, *Eur. J. Inorg. Chem.* **2008**, 5439-5454. (c) Amgoune, A.; Bourissou, D. σ-Acceptor, Z-type ligands for transition metals, *Chem. Commun.* **2011**, 859-871. (d) Emslie, D. J. H.; Cowie, B. E.; Kolpin, K. B. Acyclic boron-containing π-ligand complexes: η^2- and η^3-coordination modes, *Dalton Trans.* **2012**, *41*, 1101-1117. (e) Kameo, H.; Nakazawa, H. Recent Developments in the Coordination Chemistry of Multidentate Ligands Featuring a Boron Moiety, *Chemistry-an Asian Journal* **2013**, *8*, 1720-1734.

(3) (a) Emslie, D. J. H.; Blackwell, J. M.; Britten, J. F.; Harrington, L. E. A Zwitterionic Palladium(II) η^3-Boratoxypentadienyl Complex: Cooperative Activation of Dibenzylideneacetone between Palladium and a Phosphine/Thioether/Borane Ligand, *Organometallics* **2006**, *25*, 2412-2414. (b) Emslie, D. J. H.; Harrington, L. E.; Jenkins, H. A.; Robertson, C. M.; Britten, J. F. Group 10 Transition Metal Complexes of an Ambiphilic PSB-Ligand: Investigations into η^3(*BCC*)-Triarylborane Coordination, *Organometallics* **2008**, *27*, 5317-5325. (c) Cowie, B. E.; Emslie, D. J. H.; Jenkins, H. A.; Britten, J. F. Diversity of Metal-Ligand Interactions in Halide (X = I, Br, Cl, F) and Halide-Free Ambiphilic Ligand Rhodium Complexes, *Inorg. Chem.* **2010**, *49*, 4060-4072. (d) D. J. H. Emslie; B. E. Cowie; S. R. Oakley; N. L. Huk; H. A. Jenkins; L. E. Harrington; Britten, J. F. A Study of M-X-BR_3 (M = Pt, Pd or Rh; X = Cl or I) Interactions in Square Planar Ambiphilic Ligand Complexes: Structural, Spectroscopic, Electrochemical and Computational Comparisons with Borane-Free Analogues, *Dalton Trans.* **2012**, *41*, 3523 - 3535. (e) Cowie, B. E.; Emslie, D. J. H. Bridging Rhodium-Iron Borataaminocarbyne Complexes Formed by Intramolecular Isonitrile-Borane Coordination, *Organometallics* **2013**, *32*, 7297-7305. (f) Cowie, B. E.; Emslie, D. J. H. Bis-Hydrocarbyl Platinum(II) Ambiphilic Ligand Complexes: Alkyl–Aryl Exchange Between Platinum and Boron, *Organometallics* **2015**, *34*, 2737–2746. (g) Cowie, B. E.; Emslie, D. J. H. M–H–BR_3 and M–Br–BR_3 Interactions in Rhodium and Nickel Complexes of an Ambiphilic Phosphine-Thioether-Borane Ligand, *Can. J. Chem.* **2018**, *96*, submitted.

(4) Cowie, B. E.; Emslie, D. J. H. Platinum Complexes of a Borane-Appended Analogue of 1,1 '-Bis(diphenylphosphino)ferrocene: Flexible Borane Coordination Modes and in situ Vinylborane Formation, *Chem. Eur. J.* **2014**, *20*, 16899-16912.

(5) Cowie, B. E.; Emslie, D. J. H. Nickel and Palladium Complexes of Ferrocene-Backbone Bisphosphine-Borane and Trisphosphine Ligands, *Organometallics* **2015**, *34*, 4093-4101.

(6) Cowie, B. E.; Tsao, F. A.; Emslie, D. J. H. Synthesis and Platinum Complexes of an Alane-Appended 1,1 '-Bis(phosphino)ferrocene Ligand, *Angew. Chem. Int. Ed.* **2015**, *54*, 2165-2169.

(7) (a) Bebbington, M. W. P.; Bontemps, S.; Bouhadir, G.; Bourissou, D. Photoisomerizable Heterodienes Derived from a Phosphine Borane, *Angew. Chem. Int. Ed.* **2007**, *46*, 3333-3336. (b) Bontemps, S.; Gornitzka, H.; Bouhadir, G.; Miqueu, K.; Bourissou, D. Rhodium(I) Complexes of a PBP Ambiphilic Ligand: Evidence for a Metal→Borane Interaction, *Angew. Chem. Int. Ed.* **2006**, *45*, 1611-1614.

(8) Bontemps, S.; Bouhadir, G.; Dyer, P. W.; Miqueu, K.; Bourissou, D. Quasi-Thermoneutral P→B Interactions within Di- and Tri-Phosphine Boranes, *Inorg. Chem.* **2007**, *46*, 5149-5151.

(9) (a) Hartwig, J. F., *Organotransition Metal Chemistry: From Bonding to Catalysis*, University Science Books: Sausalito, California, 2010. (b) Crabtree, R. H., *The Organometallic Chemistry of the Transition Metals*, 3rd ed.; John Wiley & Sons: Toronto, 2001. (c) Nolan, S. P.; de la Vega, R. L.; Hoff, C. D. Thermochemical Study of the Lewis Acid Promoted Carbonyl Insertion Reaction, *J. Am. Chem. Soc.* **1986**, *108*, 7852-7853. (d) Hazari, A.; Labinger, J. A.; Bercaw, J. E. A Versatile Ligand Platform that Supports Lewis Acid Promoted Migratory Insertion, *Angew. Chem. Int. Ed.* **2012**, *51*, 8268-8271. (e) West, N. M.; Labinger, J. A.; Bercaw, J. E. Heterobimetallic Complexes of Rhenium and Zinc: Potential Catalysts for Homogeneous Syngas Conversion, *Organometallics* **2011**, *30*, 2690-2700.

(10) For pioneering examples of metal carbonyl ambiphilic/amphoteric ligand chemistry using phosphine-alane ligands, see: (a) Labinger, J. A.; Miller, J. S. Amphoteric Ligands. 1. Facile Acyl Formation and Crystal Structure of a Novel Complex Containing an η^2(C,O)-

Acylphosphonium Ligand, *J. Am. Chem. Soc.* **1982**, *104*, 6856. (b) Grimmett, D. L.; Labinger, J. A.; Bonfiglio, J. N.; Masuo, S. T.; Shearin, E.; Miller, J. S. Amphoteric Ligands. 2. Formation and Structure of a Novel C-H Bond Containing Product from $HMn(CO)_5$ and an Amphoteric Ligand, *J. Am. Chem. Soc.* **1982**, *104*, 6858. (c) Labinger, J. A.; Bonfiglio, J. N.; Grimmett, D. L.; Masuo, S. T.; Shearin, E.; Miller, J. S. Amphoteric Ligands. 3. Reactions of Alkylmetal Carbonyls with (Aluminoamion)phosphine Ligands. Structure of $(\eta\text{-}C_5H_5)(CO)Fe(C(CH_3)OAl(C_2H_5)2N(C(CMe_3)_3)P(C_6H_5)_2)$, *Organometallics* **1983**, *2*, 733. (d) Grimmett, D. L.; Labinger, J. A.; Bonfiglio, J. N.; Masuo, S. T.; Shearin, E.; Miller, J. S. Amphoteric Ligands. 4. Reactions of $HMn(CO)_5$ with (Aluminoamino)phosphine Ligands. Structure of $(CO)_3Mn[CHOAl(CH_3)_2N(C(CH_3)_3)P(C_6H_5)_2]\text{-}[P(C_6H_5)_2N(C(CH_3)_3)Al(HCH_2)(CH_3)]$, *Organometallics* **1983**, *2*, 1325.

(11) Kaufmann, L.; Breunig, J. M.; Vitze, H.; Schodel, F.; Nowik, I.; Pichlmaier, M.; Bolte, M.; Lerner, H. W.; Winter, R. F.; Herber, R. H.; Wagner, M. Electronic communication in oligonuclear ferrocene complexes with anionic four-coordinate boron bridges, *Dalton Trans.* **2009**, 2940-2950.

(12) Siewert, I.; Fitzpatrick, P.; Broomsgrove, A. E. J.; Kelly, M.; Vidovic, D.; Aldridge, S. Probing the influence of steric bulk on anion binding by triarylboranes: comparative studies of $FcB(o\text{-}Tol)_2$, $FcB(o\text{-}Xyl)_2$ and $FcBMes_2$, *Dalton Trans.* **2011**, *40*, 10345-10350.

(13) Bebbington, M. W. P.; Bontemps, S.; Bouhadir, G.; Hanton, M. J.; Tooze, R. P.; van Rensburg, H.; Bourissou, D. A 1,1 '-ferrocenyl phosphine-borane: synthesis, structure and evaluation in Rh-catalyzed hydroformylation, *New J. Chem.* **2010**, *34*, 1556-1559.

(14) Scheibitz, M.; Bolte, M.; Bats, J. W.; Lerner, H.-W.; Nowik, I.; Herber, R. H.; Krapp, A.; Lein, M.; Holthausen, M. C.; Wagner, M. $C_5H_5\text{-}BR_2$ Bending in Ferrocenylboranes: A Delocalized Through-Space Interaction Between Iron and Boron, *Chem. Eur. J.* **2005**, *11*, 584-603.

(15) Appel, A.; Jäkle, F.; Priermeier, T.; Schmid, R.; Wagner, M. Fe-B bonding in (dibromoboryl)ferrocene: A structural and theoretical investigation, *Organometallics* **1996**, *15*, 1188-1194.

(16) Carpenter, B. E.; Piers, W. E.; Parvez, M.; Yap, G. P. A.; Rettig, S. J. Synthesis, characterization and chemistry of bis(pentafluorophenyl)boryl ferrocene, *Can. J. Chem.* **2001**, *79*, 857-867.

(17) Aldridge, S.; Bresner, C. The coordination chemistry of boryl and borate substituted cyclopentadienyl ligands, *Coord. Chem. Rev.* **2003**, *244*, 71-92.

(18) Jacobsen, H.; Berke, H.; Doring, S.; Kehr, G.; Erker, G.; Frohlich, R.; Meyer, O. Lewis acid properties of tris(pentafluorophenyl)borane. Structure and bonding in $L\text{-}B(C_6F_5)_3$ complexes, *Organometallics* **1999**, *18*, 1724-1735.

(19) Jennifer Burt; James W. Emsley; William Levason; Gillian Reid; Tinkler, I. S. Systematics of BX_3 and BX_2^+ Complexes (X = F, Cl, Br, I) with Neutral Diphosphine and Diarsine Ligands *Inorg. Chem.* **2016**, *55*, 8852-8864.

(20) A valid alternative is: abstraction of a phenyl substituent from the pendent borane in FcPPB by BF_3, yielding the cationic portion of **3** paired with a BF_3Ph^- anion, followed by abstraction of F^- from BF_3Ph^- by a second equivalent of BF_3, yielding BF_4^- and BF_2Ph. However, this mechanism seems less likely, given that $B(C_6F_5)_3$ does not engage in reactivity resulting in boronium cation formation.

(21) A similar bonding description was used to describe the phosphine-coordinated borenium cation, $[(cat)B(P^tBu_3)][HB(C_6F_5)_3]$: Dureen, M. A.; Lough, A.; Gilbert, T. M.; Stephan, D. W. B–H Activation by frustrated Lewis pairs: borenium or boryl phosphonium cation?, *Chem. Commun.* **2008**, 4303.

(22) Shuttleworth, T. A.; Huertos, M. A.; Pernik, I.; Young, R. D.; Weller, A. S. Bis(phosphine)boronium salts. Synthesis, structures and coordination chemistry, *Dalton Trans.* **2013**, *42*, 12917-12925.

(23) Westcott, S. A.; Blom, H. P.; Marder, T. B.; Baker, R. T.; Calabrese, J. C. Nucleophile Promoted Degradation of Catecholborane - Consequences for Transition Metal-Catalyzed Hydroborations, *Inorg. Chem.* **1993**, *32*, 2175-2182.

(24) Müller, G.; Neugebauer, D.; Geike, W.; Köhler, F. H.; Pebler, J.; Schmidbaur, H. Bis(dimethylmethylenephosphoranyl)dihydroborato(1-) Complexes of Manganese(II) and Cobalt(II) - Stable, Homoleptic Tetraalkyls of Paramagnetic Transition-Metal Centers, *Organometallics* **1983**, *2*, 257-263.

(25) Devillard, M.; Brousses, R.; Miqueu, K.; Bouhadir, G.; Bourissou, D. A Stable but Highly Reactive Phosphine-Coordinated Borenium: Metal-free Dihydrogen Activation and Alkyne 1,2-Carboboration, *Angew. Chem. Int. Ed.* **2015**, *54*, 5722-5726.

(26) Hodgkins, T. G.; Powell, D. R. Derivatives of the dimethylbis(2-pyridyl)borate(1-) ion: Synthesis and structure, *Inorg. Chem.* **1996**, *35*, 2140-2148.

(27) de Biani, F. F.; Gmeinwieser, T.; Herdtweck, E.; Jäkle, F.; Laschi, F.; Wagner, M.; Zanello, P. Multistep redox processes and intramolecular charge transfer in ferrocene-based 2,2'-bipyridylboronium salts, *Organometallics* **1997**, *16*, 4776-4787.

(28) Denmark, S. E.; Ueki, Y. Lewis Base Activation of Lewis Acids: Group 13. In Situ Generation and Reaction of Boreniunn Ions, *Organometallics* **2013**, *32*, 6631-6634.

(29) Reactions of FcPPB with $[AuCl(SMe_2)]$, $[AuCl(PPh_3)]$ and [AuCl(CO)] afforded white, insoluble precipitates which were not further characterized.

(30) (a) Amouri, H.; Bahsoun, A. A.; Fischer, J.; Osborn, J. A.; Youinou, M. T. Synthesis and Catalytic Properties of Heterobimetallic Complexes of the Tripod Ligand $HC(PPh_2)_3$ - X-ray Molecular Structures of $[Rh(COD)\{HC(PPh_2)_3\}Au(PPh_3)](BF_4)_2$ and $[RhCu_2\{HC(PPh_2)_3\}_2(THF)_2(CH_3CN)_2](BF_4)_2F$, *Organometallics* **1991**, *10*, 3582-3588. (b) McWhannell, M. A.; Rosair, G. M.; Welch, A. J.; Teixidor, F.; Vinas, C. The first examples of η^5-bonding of a carbaborylphosphine ligand to transition metals. Synthesis and characterisation of $7\text{-}\{PPh_2AuPPh_3\}\text{-}8\text{-}Ph\text{-}7,8\text{-}nido\text{-}C_2B_9H_{10}$, $1\text{-}\{PPh_2AuCl\}\text{-}2\text{-}Ph\text{-}3\text{-}(p\text{-cymene})\text{-}3,1,2\text{-}pseudocloso\text{-}RuC_2B_9H_9$ and $1\text{-}\{PPh_2AuCl\}\text{-}2\text{-}Ph\text{-}3\text{-}(\eta\text{-}C_5Me_5)\text{-}3,1,2\text{-}pseudocloso\text{-}RhC_2B_9H_9$, *J. Organomet. Chem.* **1999**, *573*, 165-170.

(31) A solution of gold complex **4** did not react with carbon monoxide (1 atm, 24 h) at room temperature.

(32) (a) Barranco, E. N.; Crespo, O.; Gimeno, M. C.; Laguna, A.; Jones, P. G.; Ahrens, B. Gold and silver complexes with the ferrocenyl phosphine $FcCH_2PPh_2$ [Fc = $(\eta^5\text{-}C_5H_5)Fe(\eta^5\text{-}C_5H_4)$], *Inorg. Chem.* **2000**, *39*, 680-687. (b) Less, R. J.; Guan, B. H.; Muresan, N. M.; McPartlin, M.; Reisner, E.; Wilson, T. C.; Wright, D. S. Group 11 complexes containing the $[C_5(CN)_5]^-$ ligand; 'coordination-analogues' of molecular organometallic systems, *Dalton Trans.* **2012**, *41*, 5919-5924. (c) Bayler, A.; Schier, A.; Bowmaker, G. A.; Schmidbaur, H. Gold is smaller than silver, crystal structures of bis(trimesitylphosphine)gold(I) and bis(trimesitylphosphine)silver(I) tetrafluoroborate, *J. Am. Chem. Soc.* **1996**, *118*, 7006-7007. (d) Deák, A.; Megyes, T.; Tárkányi, G.; Király, P.; Biczók, L.; Pálinkás, G.; Stang, P. J. Synthesis and Solution- and Solid-State Characterization of Gold(I) Rings with Short Au···Au Interactions. Spontaneous Resolution of a Gold(I) Complex, *J. Am. Chem. Soc.* **2006**, *128*, 12668-12670.

(33) (a) Schmidbaur, H. Ludwig Mond lecture. High-carat gold compounds, *Chem. Soc. Rev.* **1995**, *24*, 391-400. (b) Schmidbaur, H.; Schier, A. A briefing on aurophilicity, *Chem. Soc. Rev.* **2008**, *37*, 1931-1951. (c) Schmidbaur, H.; Schier, A. Aurophilic interactions as a subject of current research: an up-date, *Chem. Soc. Rev.* **2012**, *41*, 370-412.

(34) Cordero, B.; Gómez, V.; Platero-Prats, A. E.; Revés, M.; Echeverría, J.; Cremades, E.; Barragán, F.; Alvarez, S. Covalent radii revisited, *Dalton Trans.* **2008**, 2832-2838.

(35) Bontemps, S.; Bouhadir, G.; Miqueu, K.; Bourissou, D. On the Versatile and Unusual Coordination Behaviour of Ambiphilic Ligands *o*-$R_2P(Ph)BR'_2$, *J. Am. Chem. Soc.* **2006**, *128*, 12056-12057.

(36) Sircoglou, M.; Bontemps, S.; Mercy, M.; Saffon, N.; Takahashi, M.; Bouhadir, G.; Maron, L.; Bourissou, D. Transition-metal complexes featuring Z-type ligands: Agreement or discrepancy between geometry and d^n configuration?, *Angew. Chem. Int. Ed.* **2007**, *46*, 8583-8586.

(37) Bontemps, S.; Bouhadir, G.; Gu, W.; Mercy, M.; Chen, C.-H.; Foxman, B. M.; Maron, L.; Ozerov, O. V.; Bourissou, D. Metallaboratranes derived from a triphosphanyl-borane: Intrinsic C_3 symmetry supported by a Z-type ligand, *Angew. Chem. Int. Ed.* **2008**, *47*, 1481-1484.

(38) Sircoglou, M.; Bontemps, S.; Bouhadir, G.; Saffon, N.; Miqueu, K.; Gu, W. X.; Mercy, M.; Chen, C. H.; Foxman, B. M.; Maron, L.; Ozerov, O. V.; Bourissou, D. Group 10 and 11 Metal Boratranes (Ni, Pd, Pt, CuCl, AgCl, AuCl, and Au^+) Derived from a Triphosphine-Borane, *J. Am. Chem. Soc.* **2008**, *130*, 16729-16738.

(39) Inagaki, F.; Matsumoto, C.; Okada, Y.; Maruyama, N.; Mukai, C. Air-Stable Cationic Gold(I) Catalyst Featuring a Z-Type Ligand: Promoting Enyne Cyclizations, *Angew. Chem. Int. Ed.* **2015**, *54*, 818-822.

(40) Nag, S.; Banerjee, K.; Datta, D. Estimation of the van der Waals radii of the d-block elements using the concept of bond valence, *New J. Chem.* **2007**, *31*, 832-834.

(41) Burger, B. J.; Bercaw, J. E., Vacuum Line Techniques for Handling Air-Sensitive Organometallic Compounds. In *Experimental Organometallic Chemistry - A Practicum in Synthesis and Characterization*, American Chemical Society: Washington D.C., 1987; Vol. 357, p 79-98.

(42) (a) Pohlmann, J. L. W.; Brinckmann, F. E. Pentafluorophenyl-Metal Chemistry II. Preparation and Characterization of Group IIIA Derivatives, *Z. Naturforsch. B* **1965**, *20*, 5-11. S. (b) Lancaster Alkylation of boron trifluoride with pentafluorophenyl Grignard reagent; Tris(pentafluorophenyl)boron; borane, *ChemSpider SyntheticPages* **2001**, http://cssp.chemspider.com/215.

(43) Rudie, A. W.; Lichtenberg, D. W.; Katcher, M. L.; Davison, A. Comparative study of 1,1'-bis(diphenylphosphino)cobaltocinium hexafluorophosphate and 1,1'-bis(diphenylphosphino)ferrocene as bidentate ligands, *Inorg. Chem.* **1978**, *17*, 2859.

Table of Contents artwork